Co-published by
Institute of Fluid-Flow Machinery
Polish Academy of Sciences
Committee on Thermodynamics and Combustion
Polish Academy of Sciences

http://www.imp.gda.pl/archives-of-thermodynamics/

Flame stabilization and combustion enhancement in a scramjet combustor by varying strut injection angles

Venkateshwaran Vanamamalai[a], Padmanathan Panneerselvam[a*]

[a]School of Mechanical Engineering, Vellore Institute of Technology, Vellore, Tamilnadu- 632014, India
*Corresponding author email: padmanathan.p@vit.ac.in

Received: 03.02.2024; revised: 11.06.2024; accepted: 12.06.2024

Abstract

The present study explores the characteristics of reacting flow in a scramjet combustor with struts, focusing particularly on implementing different injection strategies. A three-dimensional DLR scramjet combustor is utilised to assess the impact on the system, incorporating multiple injections and varying injection angles on the triangular wedge. The analysis considers three injectors with parallel, upward and downward injections at angles of 15° and 30°. The numerical investigation is conducted under a constant total pressure of 7.82 bar, a temperature of 340 K, and an airspeed of Mach 2 at the inlet. The results highlight the significance of injector location and shape in promoting flame stabilization. Furthermore, injection angles play a crucial role in mitigating shockwave intensity. The numerical analysis involves a steady-state Reynolds-averaged Navier-Stokes equation with the shear stress transport k–ω turbulence model. The obtained results were analyzed by examining the critical variables such as Mach number, static pressure and combustion efficiency across the combustor. Based on the computational results, injecting fuel upward not only increases the overall pressure loss but also enhances the subsonic regime downstream of the strut, which leads to better mixing and combustion efficiencies. This is primarily due to shockwave generation from the edges of the strut and the interactions with the fuel stream shear layers.

Keywords: Hydrogen fuel; Combustion efficiency; Scramjet combustor; Flame stabilization; Strut injector

Vol. 45(2024), No. 3, 167–178; doi: 10.24425/ather.2024.151227

Cite this manuscript as: Vanamamalai, V., & Panneerselvam, P. (2024). Flame stabilization and combustion enhancement in a scramjet combustor by varying strut injection angles. *Archives of Thermodynamics*, 45(3), 167–178.

1. Introduction

Scramjet engines operate as air-breathing propulsion systems, enabling them to attain hypersonic speeds while maintaining regular functionality. These engines produce thrust by compressing incoming air and combusting it with pre-existing onboard fuel, making them well-suited for efficiently propelling high-speed vehicles like missiles or aircraft. The application of scramjet engines becomes imperative for hypersonic and supersonic flight, characterized by vehicle speeds exceeding Mach 5 [1–4]. The ineffectiveness of conventional jet engines at hypersonic speeds is attributed to the challenges posed by shockwaves and increased drag. In contrast, scramjet engines outperform in high-velocity environments, given their specific design for such conditions. However, it is crucial to acknowledge that scramjet engines encounter various technological hurdles that require resolution. [5–7]. Attaining steady combustion during hypersonic speeds is a challenge due to the rapid air velocity. To address this, various geometric shapes, including cavities [8–12], struts [13–18], pylons [19–22], and shockwave generators [23,24], have been employed within the combustor. These design modifications aim to enhance mixing and combustion processes, mit-

Nomenclature

A – area of the cross-section, m^2
$\dot{m}$ – overall mass flux, kg/s
P – static pressure, Pa
P_0 – total or stagnation pressure, Pa
T – static temperature, K
u – axial velocity, m/s
X – axial distance from the inlet, m
Y – distance, m
Y – mass fraction

Greek symbols

η_C – combustion efficiency, %
η_t – total pressure loss, %
ρ – density, kg/m^3

Subscripts and Superscripts

H_2 – hydrogen
H_2O – water
N_2 – nitrogen
O_2 – oxygen

Abbreviations and Acronyms

AUSM– advection upwind splitting method
CFD – computational fluid dynamics
CFL – Courant-Friedrichs-Lewy
GIT – grid independence test
RANS– Reynolds-averaged Navier-Stokes (equations)
SST – shear stress transport

igating the difficulties associated with high-speed airflow and contributing to more effective combustion at hypersonic speeds. This phenomenon induces turbulent flow, effectively promoting the mixing of fuel and air. Consequently, it leads to an improved efficiency in the combustion process.

Effectively controlling shockwaves is a crucial consideration in the design and operation of a scramjet engine. The rapid flow of air and fuel through the combustor creates conditions that can give rise to shockwaves. These shockwaves stem from the compression and heating of incoming air, causing abrupt changes in both pressure and temperature within the engine. Shockwaves play a significant role in governing and maintaining the combustion process [25–27]. Their function involves ensuring that the air and fuel mixture remains confined within the combustor for a sufficient duration. Engineers employ diverse design strategies to mitigate the adverse effects of these factors. Intricate geometries within the combustor are often utilized to control the flow and minimize the impact of shockwaves [28,29].

Cavities are commonly integrated into scramjet combustors to enhance mixing and combustion processes. These structures induce turbulence, promoting better fuel-air mixing and, consequently, improving combustion efficiency. The incorporation of cavities contributes to an expanded surface area, thereby enhancing the combustion process. This leads to improved efficiency and accelerated fuel burning within the scramjet engine. Furthermore, cavities contribute to flame stabilization and help prevent flame blowout [30]. Li et al. [31] investigated the impact of different depths and diameters of multi-cavities on a Mach 2.52 flow. They have focused on the flow structure and mixing effectiveness at various pressure ratios across different cavity depths. The study revealed that increasing cavity depth and utilizing multiple cavities with a maximum number of injections could lead to improved mixing compared to a single injection. This improvement is attributed to the generation of shock waves and the separation of the shear layer. Jeyakumar et al. [32] experimentally examined cavity-based reacting and non-reacting flow in circular cross sectional combustor. They tested various cavity configurations such as fore wall modifications [33], aft wall angles with single and dual step angles [34], various cavity depths [35], and transverse upstream injection [36] within the scramjet combustor. Their findings demonstrate that employing transverse upstream injection with aft wall angle cavities results in lower stagnation pressure loss compared to rectangular cavities. Additionally, they observed uniform mixing with increasing injection pressures.

Kannaiyan [37] examines the supersonic combustion of ethylene was investigated in various combustor configurations, including the baseline design without a cavity, a configuration featuring a square cavity, and another with an angled cavity. The findings unequivocally show that the model combustor, distinguished by a shallow and sloped aft-wall cavity, exhibits the longest residence period and the highest level of heat release. Moreover, it is noted that the influence of a cavity with a reduced length-to-depth ratio on the estimation of residence time and heat release is negligible. The research conducted by Liu et al. [38] investigated the application of cavity-based scramjet engines in both counter-jet and co-jet configurations. The study's results indicate that the counter-jet configuration has a more pronounced impact on fuel mixing compared to the co-jet configuration. This effect is attributed to the proximity of the main eddy to the counter jet, facilitating an efficient distribution of fuel through the primary circulation. The findings suggest that the penetration of hydrogen in counter jets is approximately 25% higher compared to co-jets. Feng et al. [39] conducted research on the combustion behaviors of powder fuels within a cavity-based supersonic combustion chamber. The findings suggest that steady burning of the powder fuel is achievable in the presence of supersonic wind. The main areas of flame dispersion occur within the cavity's interior and the shear layer, near the boundary layer of the expansion region. As the air-to-fuel ratio increases, the total pressure loss beside the combustion chamber decreases. However, the efficiency of powder particle combustion exhibits the opposite trend. In the cavity-based supersonic combustor, reducing the amount of air to fuel mixture proves advantageous.

An experimental investigation was conducted on a combined fuel injection method involving a strut/wall configuration by Qiu et al. [40]. The primary goal of this investigation was to improve the combustion performance in a flush-wall scramjet combustor fueled with liquid kerosene. The results suggest that the combustion intensity of the core flame increases with a higher fuel equivalency ratio. The combustion process includes the

propagation of the core flame toward the combustor sidewall, igniting the fuel present on the wall, and leading to the formation of a wall flame. The presence of the wall flame induces thermal choking downstream of the strut, thereby enhancing the flame within the core. The performance of the combustor and the characteristics of the flame are influenced by the different fuel distribution strategies employed. Additionally, the positioning of wall fuel injectors is optimized to enhance combustion efficiency. Steady and unsteady flow characteristics of strut-based scramjet combustors with implications of the dual cavity and various cavity locations were analyzed numerically by Rajesh et al. [41,42], Athithan et al. [43] and Jeyakumar et al. [44]. The results reveal that the dual cavity is shifted away from the strut injector, and a lateral expansion of the combustion zone is observed. This phenomenon improves combustion propensity and facilitates a decrease in combustor length.

Flame propagation characteristics and combustion performance with multiple struts and fueled by liquid kerosene were examined by Qiu et al. [45]. The study concentrated on examining fuel distribution patterns, particularly investigating different single-strut injection methods and expanding the analysis to include up to five injection struts. The findings demonstrated an enhancement in fuel mixing efficiency, reaching a value of 53.8%, with an increase in the number of injection struts. The discussion revolved around the interaction that occurs between the flame of the ignition and injection struts. A technique for augmenting the width of flame spread, without the need for additional energy input, was suggested, drawing upon the inherent properties of flame propagation. Kummitha et al. [46] concentrated on analyzing wedge-shaped and revolved wedge-shaped injectors to explore the possibility of improving mixing by increasing interactions between the shear mixing layer and shock wave. The results indicate that the newly designed struts achieved complete mixing at a distance of 0.180 m from the combustor inlet. This accomplishment was accompanied by an average gain in mixing efficiency of 9%, with a corresponding increase in pressure losses of 12%.

Much of the research on strut combustor scramjets has primarily focused on a single injector located at the central strut. While numerous studies have reported numerical results using a two-dimensional scramjet combustor with a strut, the development of three-dimensional scramjet combustors has lagged. This current work addresses supersonic flows at high speeds, highlighting the significant impact of a wedge on flow characteristics. The presence of a wedge contributes to the development of gradients in flow properties, including pressure, velocity, and density. This study also emphasized investigating various injection angles within the strut, to create more disruptions in the flow field and enhance diverse interactions between shear layers, shock waves, and flow streams. Understanding the flow physics associated with injection angles in strut-based supersonic flow is vital for optimizing mixing mechanisms, controlling flow characteristics, and improving the efficiency of scramjet combustion. Given that higher injection angles can significantly disrupt the boundary layer formed along surfaces, leading to increased flow separation, boundary layer instabilities, and potential impacts on combustion performance, lower injection angles were chosen for this study. The research has systematically explored the impact and importance of the injection position on mixing enrichment specifically in the context of the strut base.

2. Numerical methodology

2.1. Geometric modelling

A numerical analysis was performed on a scramjet combustor utilizing angular injection within a strut-based configuration. In this study, two distinct injection angles with three-hole injections were selected and compared against a parallel injection method. Specifically, injection angles of 15° and 30° were employed using upward and downward injection techniques. The hydraulic diameter of the injection holes for the three injection ports was consistently maintained at 1 mm. The gaseous state of hydrogen is utilized as the reactive fluid, being injected from the strut base under sonic conditions. The incoming free stream air reaches the entrance of the combustor with Mach 2. The dimensions of the scramjet model are 300 mm in length, 45 mm in breadth, and 50 mm in height. The leading edge of the strut is positioned at a distance of 68 mm from the air intake while maintaining a vertical distance of 25 mm above the bottom wall. The half angle of the strut remains constant at 6°. The length of the strut is measured at 32 mm. The upper wall features a divergence angle of 3°, starting 100 mm from the inlet of the combustor, as illustrated in Fig.1, and terminating at its outlet. The separation between the base of the strut and the entrance of the combustor measures 100 mm.

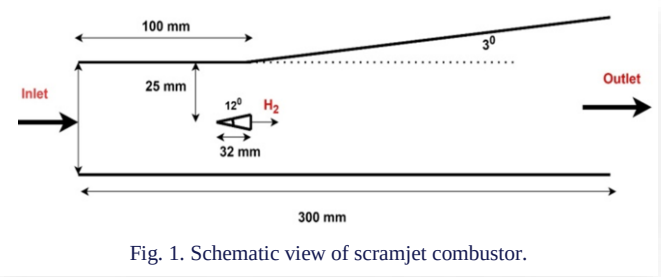

Fig. 1. Schematic view of scramjet combustor.

2.2. Numerical modelling

The study of the scramjet combustor entails solving three-dimensional conservative equations governing the conservation of mass, momentum, and energy. The primary challenge in studying supersonic flows lies in developing reliable turbulence models that allow for the examination of the underlying flow structure [47]. The current approach utilizes the Shear Stress Transport (SST) k–ω turbulence model to solve the compressible Reynolds-averaged Navier-Stokes (RANS) equations. The k–ω SST model is considered the most accurate turbulence model for scramjets [48]. It enables predictions of mixing layers, negative pressure gradients, and separated flows, making it suitable for a comprehensive analysis of scramjet flows [49]. In the ANSYS Fluent framework [50], the finite volume approach is employed to discretize the governing equations of the flow. The modelling of the working fluid as an ideal gas, along with the use of a mix-

ing-law equation, allows for the capture of both density and viscosity fluctuations. The combination of the Advection Upwind Splitting Method (AUSM) with a higher-order upwind approach enhances convergence and yields more accurate results [51]. Ensuring stability involves preventing divergence and maintaining the Courant-Friedrichs-Lewy (CFL) value at 0.5 [52], providing a reliable approach to guarantee a stable solution.

2.3. Discretization and grid independence test

The three-dimensional grid generation for the strut-based scramjet combustor was completed using Ansys ICEM R22, employing hexahedral elements. The O-Grid method was utilized to discretize the injectors, enabling the creation of structured grids closely aligned with the geometry to ensure an accurate representation of the flow domain. To capture shockwaves and boundary layer interactions effectively, the y+ value is kept below 1 near the wall boundaries. Additionally, the grid elements are maintained with a minimum angle of approximately 45° and a skewness of around 0.9 to ensure optimal grid quality. A grid independence test is essential to ensure computational consistency. To enhance the accuracy of numerical results while minimizing computational cost and time, three different element sizes were employed to optimize grid resolution. Grid independence test (GIT) was conducted on a three-dimensional supersonic combustor, employing three different mesh element sizes: 3.5 million, 6.6 million, and 9.9 million elements. The discretized 3D scramjet combustor and zoomed view of the O-Grid mesh is depicted in Fig. 2.

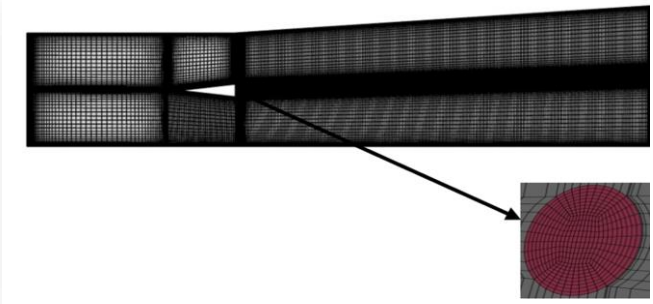

Fig. 2. Three-dimensional mesh of the scramjet combustor.

The investigation involved measuring total pressure and Mach number along the centerline of the combustor. Figures 3a and 3b illustrate minimal variation among the three mesh element sizes concerning both the bottom wall pressure and axial pressure plots. To minimize convergence time, medium size mesh elements were selected for this investigation.

2.4. Boundary conditions

The steady-state three-dimensional modeling of the strut-based scramjet combustor employs specific boundary conditions were shown in Table 1.

Table 1. Inlet boundary conditions for air and fuel.

Condition	Air	Hydrogen
Mach number	2.0	1.0
Velocity	730 m/s	1200 m/s
Density (ρ)	1.002 kg/m^3	0.097 kg/m^3
Static pressure (P)	100 000 Pa	100 000 Pa
Total or stagnation pressure (P_0)	782 444 Pa	189 292 Pa
Static temperature (T)	340 K	250 K
Mass fraction of hydrogen (Y_{H2})	0	1
Mass fraction of water (Y_{H2O})	0.032	0
Mass fraction of oxygen (Y_{O2})	0.232	0
Mass fraction of nitrogen (Y_{N2})	0.736	0

The static pressure and Mach number of the entering airflow have been provided, making the far-field the definition for air and fuel inlet. Due to the density-based solver, the operating conditions were stated to be zero. For the walls of the combustor and the strut, a no-slip wall condition has been defined. The outlet from the combustor is characterized by a pressure outlet.

2.5. Combustion modelling

In the context of investigating the combustion characteristics of supersonic flow, the computational analysis incorporates the utilization of species transport [53] and eddy dissipation models. The utilization of the eddy dissipation concept is employed as a means to streamline the complex connections between turbulence and chemistry, while also aligning with empirical observations [54]. The selection of a single-step reaction process over multistep hydrogen reaction models is based on the superior outcomes it offers in terms of overall combustor performance. The utilization of a single-step reaction mechanism has the added benefit of reducing the computational period required for solving the reaction equation [55]:

$$2H_2 + O_2 \rightarrow 2H_2O. \quad (1)$$

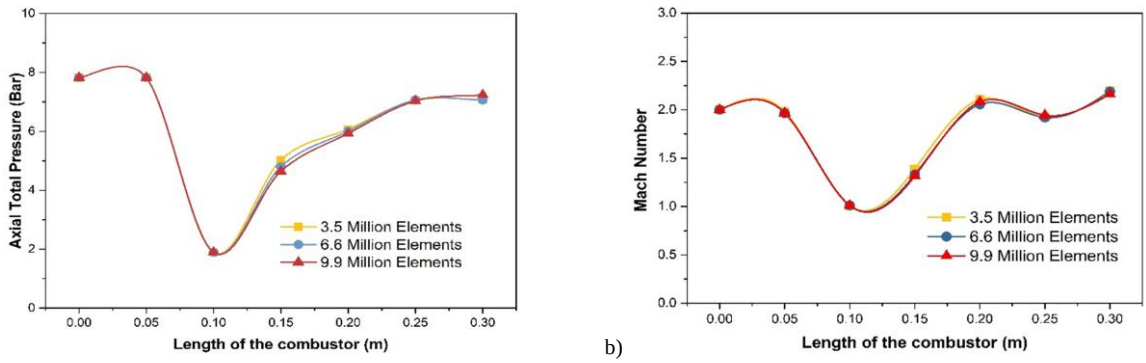

a) b)

Fig. 3. Grid independence study: a) static pressure along the bottom wall of the combustor, b) axial pressure along the centerline of the combustor

2.6. Validation

The assessment of the steady-state simulation results involved a comparative analysis carried out by Oevermann [47] at the DLR (German Aerospace Center) scramjet combustor. The present study has been validated for both reacting and non-reacting conditions. In the non-reacting conditions, the analysis includes the consideration of static pressure at the bottom wall and centerline. In contrast, for reactive cases, the study demonstrates the distribution of velocity magnitude and temperature. From Figs. 4 a and b, the observed agreement between the simulation outcomes and empirical data includes consistent findings related to strut-generated shock, wall-reflected shock waves, and the distribution of wall static pressure. The observed slight fluctuations in static pressure near the boundary may be attributed to unexpected turbulence vortices close to the wall. The numerical results exhibit a similar pattern and only marginal variation when compared with experimental observations.

The validation process for reacting flows encompasses considerations of combustion chemistry, incorporating the eddy dissipation model, and solving species transport equations. The velocity distributions at X = 78 mm, X = 125 mm, and X = 207 mm along the axial plane are depicted in Figs. 5a to 5c.

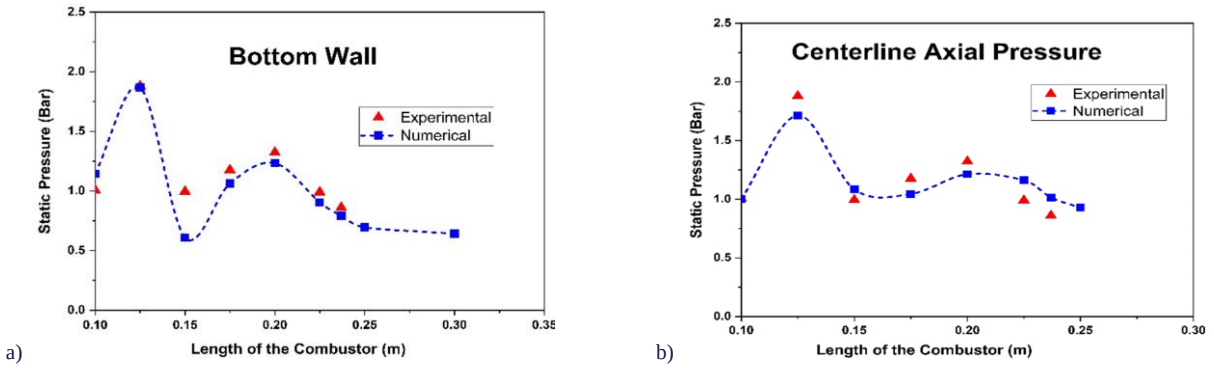

Fig. 4. Validation for 3-dimensional scramjet combustor using pressure plots (non-reacting): a) static pressure at bottom wall, b) static pressure at a distance of Y = 25 mm.

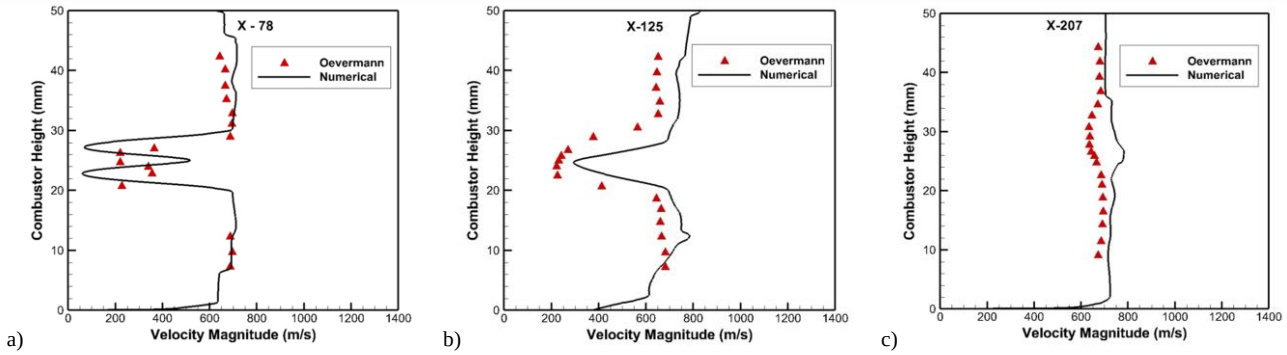

Fig. 5. Validation of axial velocity plots for reacting flow with Oevermann [47] at: a) X = 78 mm, b) X = 125 mm, c) X = 207 mm.

The comparison reveals a high level of concordance between experimental findings and numerical simulations, with minimal discernible deviation. Figures 6a to 6c illustrates the temperature distribution along the strut-based scramjet combustor at axial positions of X = 78 mm, X = 125 mm and X = 233 mm from the inlet. The numerical predictions closely align with experimental observations. Discrepancies between the high-temperature values obtained in experiments and those predicted numerically can be attributed to heat transfer effects and three-dimensional vortices. Nevertheless, the study demonstrates the competence of the numerical approach employed here in analyzing diverse configurations of strut-based scramjet combustors.

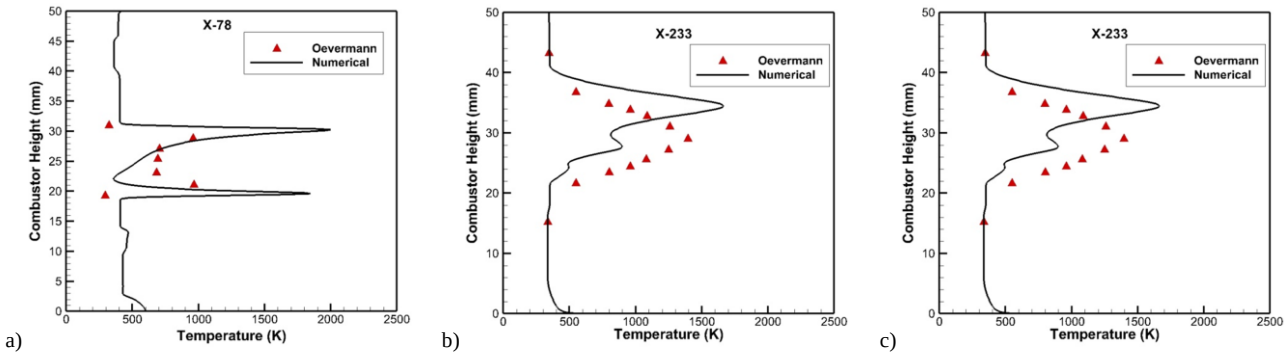

Fig. 6. Validation of static temperature with Oevermann [47] at: a) X = 78 mm, b) X = 125 mm, c) X = 233 mm.

3. Results and discussion

In this study, computational fluid dynamics (CFD) is employed for numerical analysis to investigate the mixing performance associated with different strut injection techniques in the DLR scramjet combustor. The primary objective is to assess the performance characteristics of a strut-based scramjet combustor under varying injection angles and directions. A recently updated three-dimensional numerical investigation further explores the impact of angled injectors, pointing both above and downward, on the overall performance of a strut-based scramjet engine. The numerical solution for steady-state flow under identical operational variables and boundary conditions is obtained by solving the RANS equations.

The density contours for different injection angles, both upward and downward configurations, are illustrated in Figs.7a to 7e, respectively.

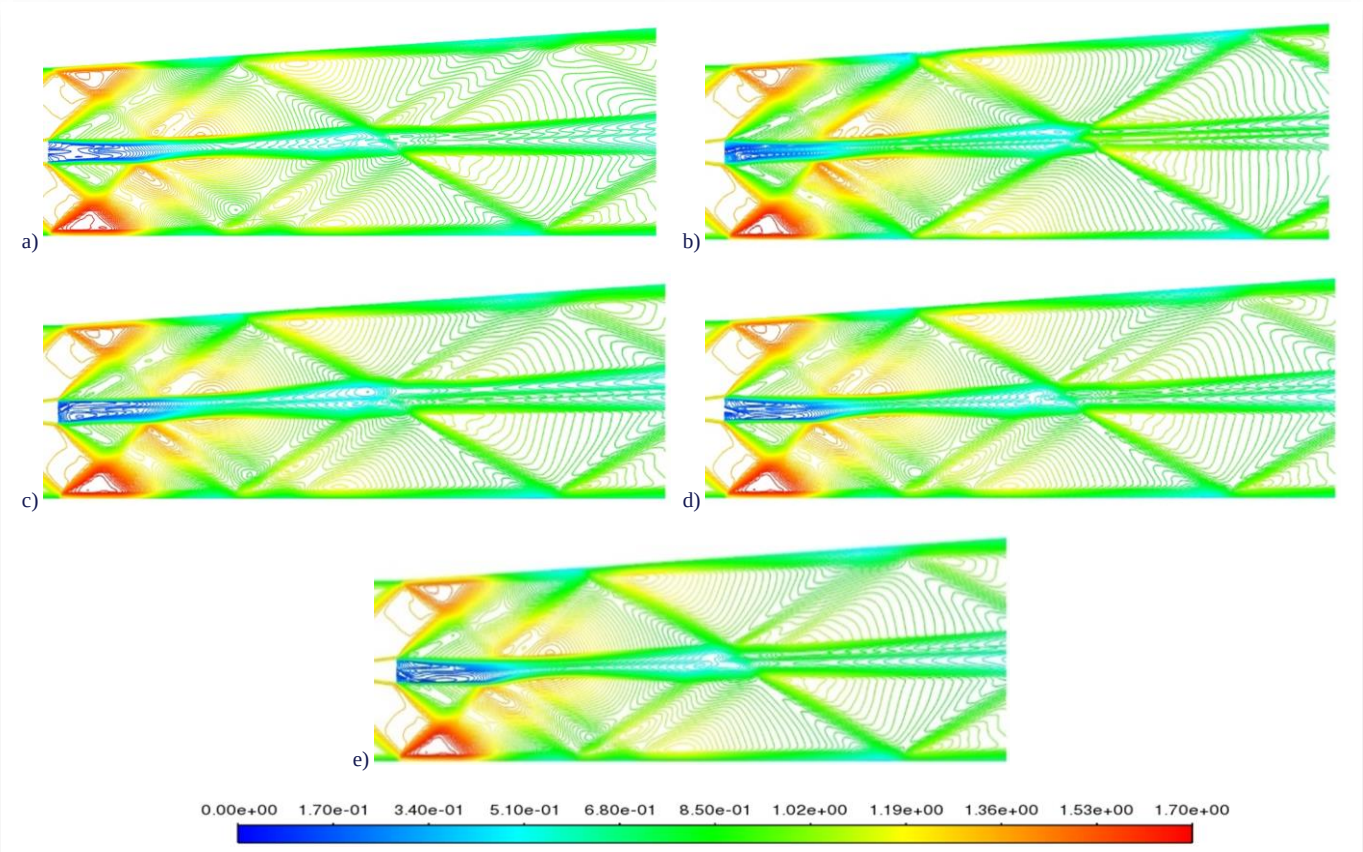

Fig. 7. Contours of density in kg/m³: a) parallel injection, b) 15° upward injection, c) 30° upward injection, d) 15° downward injection, e) 30° downward injection.

An *XY* plane has been established at the center of the combustor to visualize density and Mach number contours for four distinct injection methods: 15° upward, 15° downward, 30° upward, and 30° downward. These injections induce shockwave interactions and recirculation zones, significantly impacting the supersonic flow field. Notably, robust shocks originate from the leading edge of the strut and undergo reflection upon encountering the Combustor wall. Subsequently, these reflected shocks experience distortion at various points downstream of the strut. The shockwaves generated at the trailing edges of the strut interact with the shockwave reflected on the combustor wall, leading to a subsequent reduction in strength as they approach the bottom wall of the combustor. Interestingly, it has been noted that the strength of the reflected shock wave is contingent on the injection angle, as depicted in Fig. 7. This variability is visually represented in the density contour for both injection angles and directions.

Figure 8 represents a graphical depiction of the Mach number distribution throughout the flow field, enabling the identification of regions characterized by supersonic or subsonic flow, as well as the presence of shock waves. The development of the subsonic region occurs downstream of injection struts due to the shock and shear layer interactions. This region enables the mixing of hydrogen and air, facilitating the combustion process. The width of the subsonic area was observed to expand as the injection angle was raised, as shown in Figs. 8b–8e when compared to parallel injection. A discernible L-shaped pattern was found in Figs. 8c and 8e when employing downward injection angles. Additionally, it was discovered that boundary layer separation occurred when the flow encountered the inclination of the top wall. The magnitude of the oblique shock intensifies and causes a reduction in the velocity of the fluid downstream of the strut. The presence of these recirculation zones results in the deceleration of the high velocity flow within the combustor, hence causing a decrease in the Mach number of the combustor as measured along its length.

3.1. The effect of wall-static pressure

The graphical representation in Fig. 9a and 9b depicts the static pressure distribution along the bottom wall and axis of the combustor. Notably, the pressure levels observed at the inlet of the combustor consistently exhibited a high degree of uniformity.

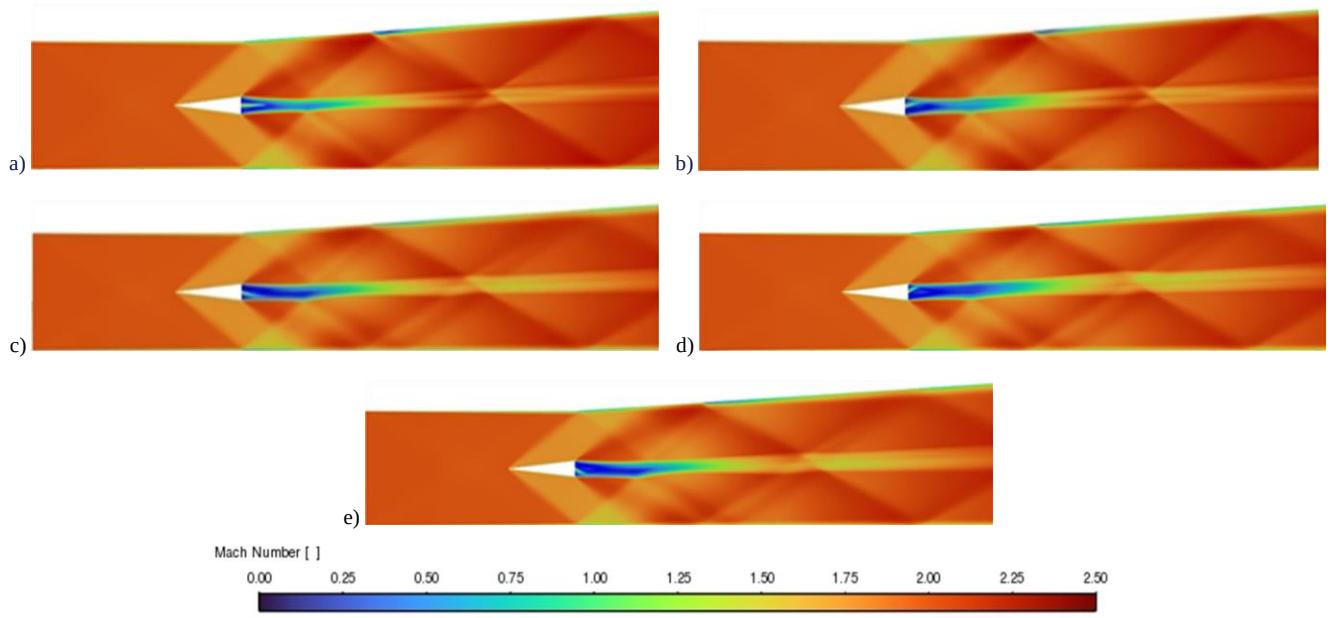

Fig. 8. Mach contours (a) Parallel injection (b) 15^0 Upward injection (c) 15^0 Downward injection (d) 30^0 Upward injection (e) 30^0 Downward injection.

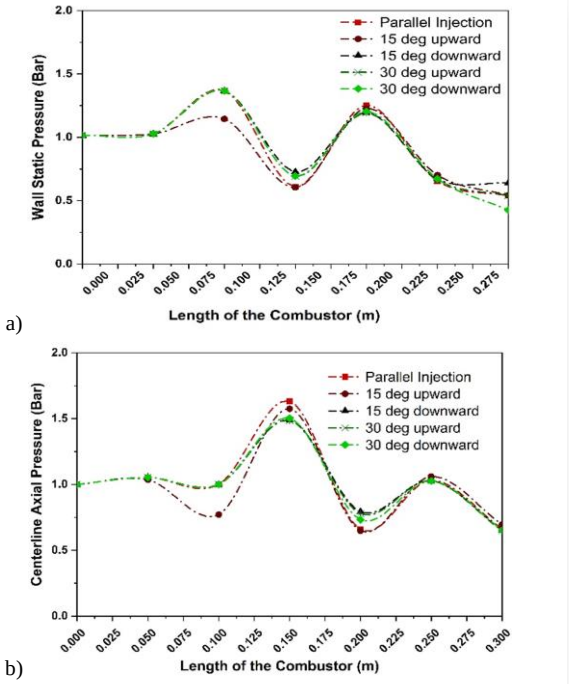

Fig. 9. Static pressure distribution for different injection angles: a) wall static pressure, b) axial pressure.

In Fig. 9a, the representation shows the static pressure exerted by the bottom wall of the combustor. Notably, as the waves developed, the pressure at a distance of 0.15 m from the leading edge of the strut decreased. An interesting observation is the significant recirculation generated at the trailing edge of the strut, stemming from upstream injection at a distance of 0.2 m, indicating the presence of elevated pressure levels. Remarkably, the range of pressures at the exit of the combustor remained consistent for both injections with varying angles.

Figures 9a and 9b highlight a significant difference in the static pressure applied to the wall by distinct configurations of struts. Axial pressure measurements were taken using the centerline of the combustor as a reference point. Notably, a higher pressure was observed at a distance of 0.15 m, attributable to the injection pressure at the midpoint of the strut. Comparing angled injection to parallel injection, it is evident that angled injection leads to a higher pressure exerted at the center of the combustor compared to the center of the strut. The presence of the recirculation area located in the central region of the strut base, as depicted in Fig. 9b for the 15° upward injection, leads to a higher injection pressure compared to the other two scenarios.

3.2. Static temperature

Temperature graphs in a scramjet combustor commonly depict the spatial distribution of temperature along the longitudinal or vertical axis of the combustor. The presented charts offer valuable insights into the combustion process and the spatial distribution of temperature for different injection angles within the combustor. From Fig. 10, it is observed that in each case at X = 128 mm, the static temperature profile exhibits a high degree of similarity, indicating a reduced level of combustion and mixing of air and fuel near the injection area when compared to the outer regions of the streams. In all instances, it can be observed that at X = 128 mm, the temperature profile exhibits a high degree of similarity, indicating a reduced level of mixing and combustion of the fuel and air near the injection site in comparison to the boundary of the streams. Additionally, it can be noted that as the flow progresses towards the exit of the combustor, there is a reduction in temperature along the axial distance from the inlet at X = 175 mm, X = 207 mm, and X = 283 mm. The DLR scramjet model exhibits a concentration of maximum temperature within

the central region of the combustor. The subsonic zone is where intense combustion occurs as a result of the intense interactions between shock waves and the fuel shear layer. Additionally, the flow downstream is decelerated due to shock-shock interactions. Furthermore, the interaction between the fuel-air stream and the strut injector occurs at a location further downstream. The highest recorded temperature was obtained at a distance of X = 128 mm from the combustor inlet. This finding is further substantiated by the presented data in Figs. 10a to 10d, where the peak temperature was observed within the range of Y = 0.20 mm to Y = 0.35 mm.

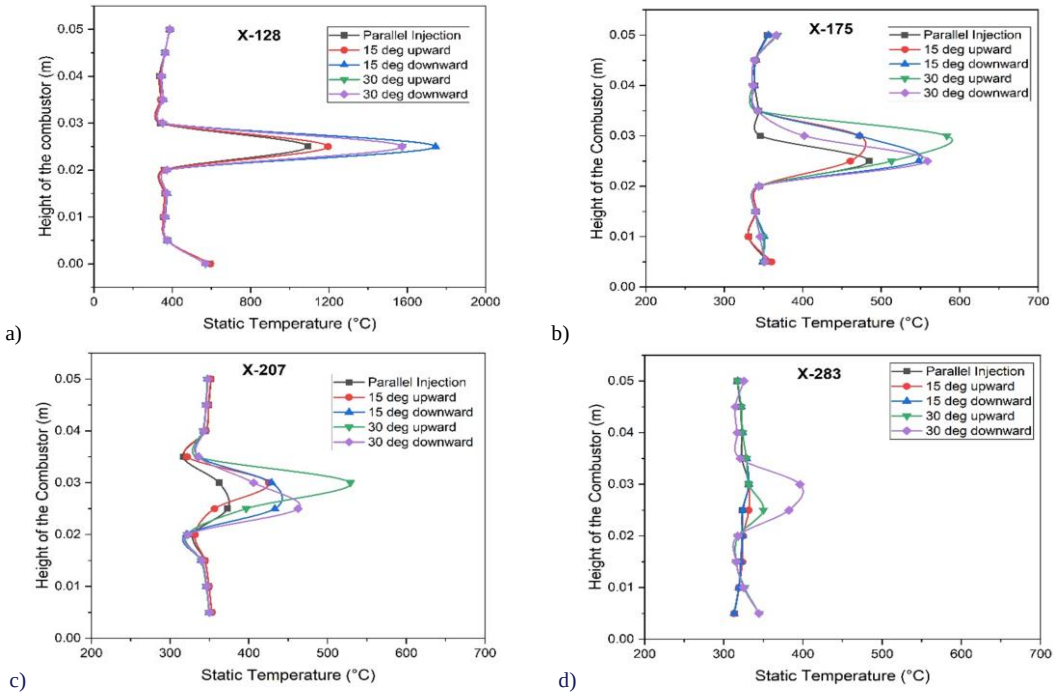

Fig. 10. Temperature profile along the combustor at a distance of: a) X = 128 mm, b) X = 157 mm, c) X = 207 mm, d) X = 283 mm.

3.3. Performance analysis

3.3.1. Combustion efficiency

The most crucial variables for achieving optimal performance in scramjet combustors are the efficiency of mixing and combustion. The air-fuel mixing efficiency of any position across the stream can be determined by calculating the average values and expressing it as the ratio of the stoichiometric hydrogen mass flux to the overall hydrogen mass flux. This representation is as follows[56]:

$$\eta_C = 1 - \frac{\int A(X)\rho_{gas} u Y_{H_2} dA}{\dot{m}_{H2(inj)}} = 1 - \frac{\dot{m}_{H2(X)}}{\dot{m}_{H2(inj)}}, \qquad (2)$$

where Y_{H2} stands for the hydrogen mass percentage and gas density, while A represents the area of the cross-section. Additionally, u indicates the axial velocity. Assuming that $\dot{m}_{H2(inj)}$ signifies the overall hydrogen mass flux and $\dot{m}_{H2(X)}$ the hydrogen mass flux about X.

Figure 11a illustrates the fluctuation in the combustion efficiency of the DLR scramjet model as a function of various injection angles. The phenomenon of shockwave and fuel stream shear layer interaction is observed to occur predominantly in the downstream region of the strut.

The existence of a subsonic region near the strut area enhances the mixing process, contributing to an overall improvement in combustion efficiency. One more observation is noted, comparing all cases with parallel injection, 15° upward injection having complete combustion attained with minimum combustor length nearly x = 0.11 m.

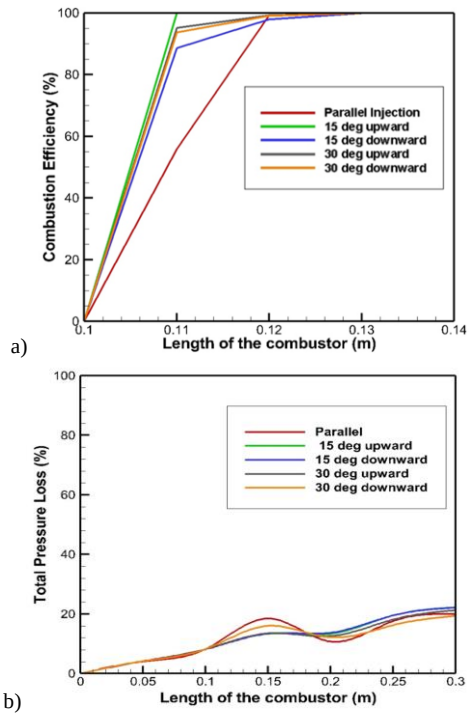

Fig. 11. (a) Combustion efficiency, and (b) total pressure loss of strut-based scramjet combustor with various injection angles.

3.3.2. Total pressure loss

Another important analysis to access the scramjet combustor performance is the total pressure loss. Illustrated in Fig. 11b is the total pressure loss corresponding to different angles of injection utilized within a strut-based scramjet combustor along its axial length. The fluctuations in pressure loss are attributed to the generation of shockwaves originating from the strut. The total pressure loss is calculated using the formula outlined below [47]:

$$\eta_t = 1 - \frac{\int_A P_0 \rho u dA}{\int_A P_{0(\text{inlet})} \rho u dA}. \quad (3)$$

Comparatively, angled injections in the scramjet combustor result in higher total pressure losses than parallel injections due to the increased strength of shockwaves. Notably, higher pressure loss is evident downstream of the strut during angled injection, primarily attributed to multiple shockwaves and their interactions with the fuel stream shear layer that decelerate the flow in the combustor. Specifically, a significant increase in pressure loss of approximately 20% is observed for upward injection angle, stemming from augmented shear layer formation and the emergence of recirculation zones in the downstream region. Additionally, an intriguing trend emerges from the Fig. 11b total pressure loss exhibits a notable decrease with increasing injection angle when compared to parallel injection configurations.

3.4. H_2 and H_2O mass fraction

The estimation of mixing and combustion characteristics for the strut-based scramjet combustor is based on the mass fractions of H_2 and H_2O in its distribution. If the combustion conditions are optimized to achieve complete combustion, the mass fraction of hydrogen can drop. Figs. 12a and 12b illustrate the mass percent of hydrogen and H_2O over the length of the combustor. A range of mass fraction variation was recorded within the distance range of 0.1 m to 0.15 m from the entrance of the combustor. Based on the findings depicted in Fig. 10a, it can be observed that optimizing the combustion conditions for achieving complete combustion may result in a drop in the hydrogen mass fraction. Figure 13 illustrates the concentration of H_2 and H_2O, expressed as mass fractions, at different axial locations within the combustor.

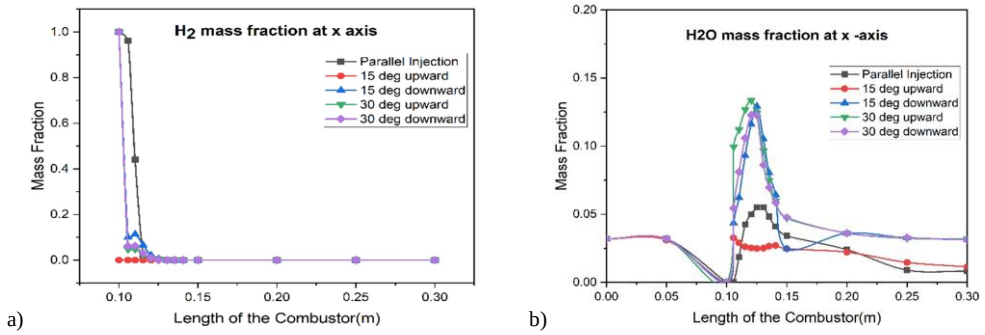

Fig. 12. Mass fraction along the length of the combustor: a) H_2 mass fraction, b) H_2O mass fraction.

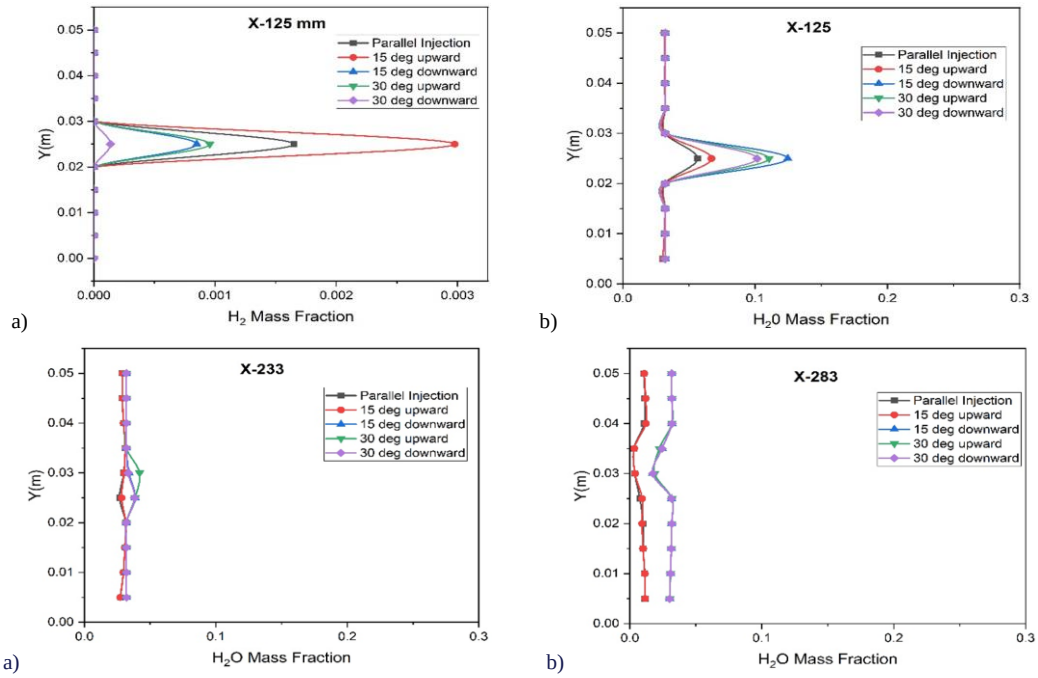

Fig. 13. H_2 and H_2O distribution at the crosswise locations of the combustor: a) H_2 mass fraction at X = 125 mm, b) H_2O mass fraction at X = 125 mm, c) H_2O mass fraction at X = 207 mm, d) H_2O mass fraction at X = 283 mm.

Figure 13 displays a discernible disparity in the H_2 mass fraction, which is found to be at a low concentration, and the H_2O mass fraction, which exhibits a substantially greater profile, specifically at the position X = 125 mm. Therefore, the implementation of angled injection in the scramjet combustor enhances combustion efficiency. The hydrogen is nearly depleted at X = 207 mm and X = 283 mm. The results of the investigation indicate that the mass fraction of H_2O is significantly higher when employing a downward injection angle at the position X =125 mm. The H_2O mass fraction graphs reveal that a similar large variation was seen in the strut wake zone. As indicated by the mass fraction graphs, it is evident that the implementation of angled injection results in the nearly complete consumption of fuel.

4. Conclusion

The numerical investigation of the three-dimensional DLR combustor is conducted and subsequently compared with experimental data. The injection of hydrogen fuel is accomplished by the utilization of a strut-type injector, which employs a range of injection angles in the direction of flow. The computational simulations employed in this study are based on the three-dimensional RANS equations. The simulations utilize the SST $k–\omega$ model to accurately predict the effects of turbulence. Additionally, the eddy-dissipation approach is employed to represent the single-step hydrogen reaction in the reacting flow. The analysis of the combustor includes an assessment of flow characteristics such as shock waves, static pressure and temperature distributions, mass fraction of hydrogen and steam, and performance parameters at different locations. The present study yields the following findings:

- From density contours, the shock interaction within the combustor led to the creation of strong recirculation zones along both the upper and lower walls. These recirculation zones play a vital role in aiding the mixing process and fostering the stabilization of the flame. The rise in pressure is ascribed to the interaction between shock waves and the separation of the boundary layer. Consequently, the downstream flow undergoes a deceleration, accompanied by a decrease in the intensity of the shocks.
- The hydrogen mass fraction profile exhibited a peak at X = 0.125 m, indicating improved mixing and combustion efficiency. This suggests that angled injection enhances the effectiveness of the scramjet combustor. The H_2 mass fraction exhibits near-complete consumption at X = 0.207 m and X = 0.283 m, indicating efficient fuel utilization. H_2O mass fraction is maximum while using of downward injection angle at X = 0.125 m. From mass fraction graphs, it can be observed that the fuel is completely burnt before it leaves the scramjet combustor.
- It is evident that upward injection angles yield superior mixing characteristics in comparison to downward injections. Notably, the subsonic region near the strut which enhances the mixing and combustion efficiencies, and angled injections, particularly upward ones, demonstrate enhanced combustion characteristics within the region of X = 0.12 m.
- The total pressure loss is higher for upward injection angles than parallel and downward injection, primarily due to shockwave generation from the leading edge of the struts. In this study, it's observed that the total pressure loss for upward injection angles is 20% and downward injection angles exhibit a 15%. It is also noted that both upward and downward injection angles have higher total pressure loss compared to parallel injection due to the emergence of additional shockwaves downstream of the strut. Despite this increased pressure loss, upward injection angles are preferred because they achieve high combustion efficiency within the shortest combustion length.

Acknowledgements

The authors are thankful to the utilization of computational facility in VIT University co-funded by the Erasmus+ Programme of the European Union, for giving the necessary permission and facilities to perform the present study.

References

[1] Curran, E.T. (2001). Scramjet engines: The first forty years. *Journal of Propulsion and Power*, 17(6), 1138–1148. doi: 10.2514/2.5875

[2] Das, N., Pandey, K.M., & Sharma, K.K. (2020). A brief review on the recent advancement in the field of jet engine - scramjet engine. In *Materials Today: Proceedings*, pp. 6857–6863. Elsevier Ltd. doi: 10.1016/j.matpr.2020.12.1035

[3] Choubey, G., Pandey, K.M., Maji, A., & Deshamukhya, T. (2017). A brief review on the recent advances in scramjet engine. In *AIP Conference Proceedings*, American Institute of Physics Inc. doi: 10.1063/1.4990189

[4] Fry, R.S. (2004). A Century of Ramjet Propulsion Technology Evolution. *Journal of Propulsion and Power*, 20(1), 27–58. doi: 10.2514/1.9178

[5] Barzegar Gerdroodbary, M., Ganji, D.D., & Amini, Y. (2015). Numerical study of shock wave interaction on transverse jets through multiport injector arrays in supersonic crossflow. *Acta Astronautica*, 115, 422–433. doi: 10.1016/j.actaastro.2015.06.002

[6] Yan, L., Wu, H., Huang, W., bin Li, S., & Liu, J. (2020). Shock wave/turbulence boundary layer interaction control with the secondary recirculation jet in a supersonic flow. *Acta Astronautica*, 173, 131–138. doi: 10.1016/j.actaastro.2020.04.003

[7] Huang, W., Tan, J.G., Liu, J., & Yan, L. (2015). Mixing augmentation induced by the interaction between the oblique shock wave and a sonic hydrogen jet in supersonic flows. *Acta Astronautica*, 117, 142–152. doi: 10.1016/j.actaastro.2015.08.004

[8] Ben-Yakar, A., & Hanson, R.K. (2001). Cavity Flame-Holders for Ignition and Flame Stabilization in Scramjets: An Overview. *Journal of Propulsion and Power*, 17 (4), 869–877. doi: 10.2514/2.5818

[9] Qiuru, Z., Huanli, Y., & Jian, D. (2021). Effects of cavity-induced mixing enhancement under oblique shock wave interference: numerical study. *International Journal of Hydrogen Energy*, 46(72), 35706–35717.

[10] Dhankarghare, A.A., Jayachandran, T., & Muruganandam, T.M. (2022). Comparative investigation of strut cavity and wall cavity in supersonic flows. *Aerospace Science and Technology*, 124, 107520. doi: https://doi.org/10.1016/j.ast.2022.107520

[11] Edalatpour, A., Hassanvand, A., Gerdroodbary, M.B., Moradi, R., & Amini, Y. (2019). Injection of multi hydrogen jets within cavity flameholder at supersonic flow. *International Journal of Hydrogen Energy*, 44(26), 13923–13931. doi: 10.1016/j.ijhydene.2019.03.117

[12] Cai, Z., Wang, T., & Sun, M. (2019). Review of cavity ignition in supersonic flows. *Acta Astronautica.*, 165, 268–286. doi: 10.1016/j.actaastro.2019.09.016

[13] He, Q., Li, J., Wen, W., Ding, Y., Li, J., & Peng, C. (2023). Experimental determination and modeling of density, viscosity, and

surface tension for sulfolane + ethyl acetate and + *n*-propyl acetate. *Journal of Chemical and Engineering Data*, 68(4), 793–804. doi: 10.1021/acs.jced.2c00706

[14] Liu, C., Zhang, J., Jia, D., & Li, P. (2022). Experimental and numerical investigation of the transition progress of strut-induced wakes in the supersonic flows. *Aerospace Science and Technology*. 120, 107256. doi: 10.1016/j.ast.2021.107256

[15] An, B., Sun, M., Wang, Z., & Chen, J. (2020). Flame stabilization enhancement in a strut-based supersonic combustor by shock wave generators. *Aerospace Science and Technology*. 104, 105942. doi: 10.1016/j.ast.2020.105942

[16] Wu, K., Zhang, P., Yao, W., & Fan, X. (2019). Computational realization of multiple flame stabilization modes in DLR strut-injection hydrogen supersonic combustor. *Proceedings of the Combustion Institute. International Symposium on Combustion*, 37(3), 3685–3692. doi: 10.1016/j.proci.2018.07.097

[17] Lakka, S., Randive, P., & Pandey, K.M. (2021). Implication of geometrical configuration of cavity on combustion performance in a strut-based scramjet combustor. *Acta Astronautica*, 178, 793–804. doi: 10.1016/j.actaastro.2020.08.040.

[18] Dinde, P., Rajasekaran, A., & Babu, V. (2006). 3D numerical simulation of the supersonic combustion of H_2. *The Aeronautical Journal*, 110(1114), 773–782. doi: 10.1017/S0001924000001640

[19] Liu, Y., Sun, M., Liang, C., Yu, J., & Li, G. (2019). Flowfield structures of pylon-aided fuel injection into a supersonic crossflow. *Acta Astronautica*, 162, 306–313. doi: 10.1016/j.actaastro.2019.06.022

[20] Oamjee, A., & Sadanandan, R. (2019). Fuel injection location studies on pylon-cavity aided jet in supersonic crossflow. *Aerospace Science and Technology*, 92, 869–880. doi: 10.1016/j.ast.2019.07.021

[21] Li, Z., Barzegar Gerdroodbary, M., Sheikholeslami, M., Shafee, A., Babazadeh, H., & Moradi, R. (2020). Mixing enhancement of multi hydrogen jets through the cavity flameholder with extended pylon. *Acta Astronautica*, 175, 300–307. doi: 10.1016/j.actaastro.2020.06.002

[22] Sekar, A., Chakraborty, M., & Vaidyanathan, A. (2022). Mixing characteristics of liquid jet injected behind a curved pylon in supersonic flow. *Experimental Thermal and Fluid Science*, 134, 110570. doi: 10.1016/j.expthermflusci.2021.110570

[23] Zhang, L., Sheng, Z., & Dan, Y. (2023). Effects of sawtooth grooves on supersonic combustion. *Aerospace Science and Technology*, 136, 108223. doi: 10.1016/j.ast.2023.108223

[24] Du, Z., Huang, W., Yan, L., Chen, Z., & Moradi, R. (2019). Mixing augmentation mechanism induced by the dual injection concept in shcramjet engines. *Acta Astronautica*, 156, 1–13. doi: 10.1016/j.actaastro.2018.11.019

[25] Barzegar Gerdroodbary, M., Jahanian, O., & Mokhtari, M. (2015). Influence of the angle of incident shock wave on mixing of transverse hydrogen micro-jets in supersonic crossflow. *International Journal of Hydrogen Energy*, 40(30), 9590–9601. doi: 10.1016/j.ijhydene.2015.04.107

[26] Zuo, Q., Yu, H., Dai, J., Yan, Y., & Chen, L. (2022). Numerical study of injection strategy based on cavity combustor under oblique shock wave interference. *International Journal of Hydrogen Energy*, 47(86), 36693–36702. doi: 10.1016/j.ijhydene.2022.08.225

[27] Zhang, Y., Wang, B., Zhang, H., & Xue, S. (2015). Mixing Enhancement of Compressible Planar Mixing Layer Impinged by Oblique Shock Waves. *Journal of Propulsion and Power*, 31(1), 156–169. doi: 10.2514/1.B35423

[28] Peng, Y., Barzegar Gerdroodbary, M., Sheikholeslami, M., Shafee, A., Babazadeh, H., & Moradi, R. (2020). Mixing enhancement of the multi hydrogen fuel jets by the backward step. *Energy*, 203, 117859. doi: 10.1016/j.energy.2020.117859

[29] Li, Z., Manh, T.D., Barzegar Gerdroodbary, M., Nam, N.D., Moradi, R., & Babazadeh, H. (2020). The influence of the wedge shock generator on the vortex structure within the trapezoidal cavity at supersonic flow. *Aerospace Science and Technology*, 98(5), 105695. doi: 10.1016/j.ast.2020.105695

[30] Gruber, M.R., Baurle, R., Mathur, T., & Hsu, K.-Y. (2001). Fundamental Studies of Cavity-Based Flameholder Concepts for Supersonic Combustors. *Journal of Propulsion and Power*, 17(1), 146–153. doi: 10.2514/2.5720

[31] Li, Z., Manh, T.D., Barzegar Gerdroodbary, M., Nam, N.D., Moradi, R., & Babazadeh, H. (2020). Computational investigation of multi-cavity fuel injection on hydrogen mixing at supersonic combustion chamber. *International Journal of Hydrogen Energy*, 45(15), 9077–9087. doi: 10.1016/j.ijhydene.2020.01.096

[32] Jeyakumar, S., Balachandran, P., Indira, S., & Thillai Arasu, P. (2006). Studies on combustion in supersonic flows. *Asian Journal of Chemistry*, 18(4), 2557–2561.

[33] Jeyakumar, S., Venkateshwaran, V., Surjith, N., Karkuvel Raja, A., & Samy, G.S. (2017). Experimental Investigations on Aft Ramp Cavities with Fore Wall Modifications in Scramjet Combustors BT. *Fluid Mechanics and Fluid Power – Contemporary Research*. (pp. 1203–1212), New Delhi, Springer India.

[34] Jeyakumar, S., Balachandran, P., & Indira, S. (2006). Experimental Investigations on Supersonic Stream Past Axisymmetric Cavities. *Journal of Propulsion and Power*, 22(5), 1141–1144. doi: 10.2514/1.21024

[35] Jeyakumar S., & Jayaraman, K. (2018). Effect of finite width cavity in axisymmetric supersonic flow field. *Proceedings of the Institution of Mechanical Engineers, Part G: Journal of Aerospace Engineering*, 232(1), 180–184. doi: 10.1177/0954410016674036

[36] Assis, S.M., Jeyakumar S., & Jayaraman, K. (2019). The Effect of Transverse Injection Upstream of an Axisymmetric Aft Wall Angled Cavity in a Supersonic Flow Field. *Journal of Physics: Conference Series*, 1276. I*nternational Conference on Recent Advances in Fluid and Thermal Sciences*, 5–7 December 2018, Dubai, U.A.E. doi: 10.1088/1742-6596/1276/1/012019

[37] Kannaiyan, K. (2020). Computational study of the effect of cavity geometry on the supersonic mixing and combustion of ethylene. *Journal of Computational Science*, 47. doi: 10.1016/j.jocs.2020.101243

[38] Liu, X., Barzegar Gerdroodbary, M., Sheikholeslami, M., Moradi, R., Shafee, A., & Li, Z. (2020). Effect of strut angle on performance of hydrogen multi-jets inside the cavity at combustion chamber. *International Journal of Hydrogen Energy*, 45(55), 31179–31187. doi: 10.1016/j.ijhydene.2020.08.124

[39] Feng, Y., Luo, S., Song, J., Xia, K., & Xu, D. (2023). Numerical investigation on the combustion characteristics of aluminum powder fuel in a supersonic cavity-based combustor. *Applied Thermal Engineering*, 221, 119842. doi: 10.1016/j.applthermaleng.2022.119842

[40] Qiu, H., Zhang, J., Gao, J., Chang, J., &. Bao, W. (2021). Research on combustion performance optimization in scramjet combustor with strut/wall combined fuel injection scheme. *Aerospace Science and Technology*, 109, 106376. doi: 10.1016/j.ast.2020.106376

[41] Rajesh, A.C., Jeyakumar, S., Jayaraman, K., & Karaca, M. (2023). Steady and unsteady flow characteristics of dual cavity in strut injection scramjet combustor. *International Journal of Hydrogen Energy*, 48(72), 28174–28186. doi: 10.1016/j.ijhydene.2023.04.017

[42] Rajesh, A.C., Jeyakumar, S., Jayaraman, K., Karaca, M., & Athithan, A.A. (2023). The implications of dual cavity location in a strut-mounted scramjet combustor. *International Communications in Heat and Mass Transfer*, 145, part B, 106855. doi: 10.1016/j.icheatmasstransfer.2023.106855.A

[43] Athithan, A., Jeyakumar, S., & Poddar, S. (2021). Influence of wall mounted ramps on DLR strut scramjet combustor under non-reacting flow field. *Materials Today: Proceedings*, 56(5), 3002−doi: 10.1016/j.matpr.2021.11.347

[44] Jeyakumar, S., Kandasamy, J., Karaca, M., Karthik, K., & Sivakumar, R. (2021). Effect of hydrogen jets in supersonic mixing using strut injection schemes. *International Journal of Hydrogen Energy*, 46(44), 23013–23025. doi: 10.1016/j.ijhydene.2021.04.123

[45] Qiu, H., Lin, L., Zhang, J., Zhang, S., & Bao, W. (2023). Influence of multi-strut interaction on flame propagation and combustion performance in a large aspect ratio combustor. *Aerospace Science and Technology*, 137. doi: 10.1016/j.ast.2023.108193

[46] Kummitha, O.R., Pandey, K.M., & Padidam, A.K.R. (2021). Effect of a revolved wedge strut induced mixing enhancement for a hydrogen fueled scramjet combustor. *International Journal of Hydrogen Energy*, 46(24), 13340–13352. doi: 10.1016/j.ijhydene.2021.01.089

[47] Oevermann, M. (2000). Numerical investigation of turbulent hydrogen combustion in a SCRAMJET using flamelet modeling. *Aerospace Science and Technology*, 4(7), 463–480. doi: 10.1016/S1270-9638(00)01070-1

[48] Menter, F.R. (1994). Two-equation eddy-viscosity turbulence models for engineering applications. *AIAA Journal*, 32(8), 1598–1605. doi: 10.2514/3.12149

[49] Li, C., Chen, X., Li, Y., Musa, O., Zhu, L., & Li, W. (2019). Role of the backward-facing steps at two struts on mixing and combustion characteristics in a typical strut-based scramjet with hydrogen fuel. *International Journal of Hydrogen Energy*, 44(52). 28371–28387. doi: 10.1016/j.ijhydene.2019.09.023

[50] Aravind S., & Kumar, R. (2019). Supersonic combustion of hydrogen using an improved strut injection scheme. *International Journal of Hydrogen Energy*, 44(12), 6257–6270. doi: 10.1016/j.ijhydene.2019.01.064

[51] Choubey G., & Pandey, K.M. (2018). Effect of variation of inlet boundary conditions on the combustion flow-field of a typical double cavity scramjet combustor. *International Journal of Hydrogen Energy*, 43(16), 8139–8151. doi: 10.1016/j.ijhydene.2018.03.062

[52] Yarasai, S.S., Ravi, D., & Yoganand, S. (2022). ScienceDirect Numerical investigation on the performance and combustion characteristics of a cavity based scramjet combustor with novel strut injectors. *International Journal of Hydrogen Energy*, 48(14), 5681–5695. doi: 10.1016/j.ijhydene.2022.11.150

[53] Tu, J., Yeoh, G.H., Liu, C., & Tao, Y. (2023). *Computational fluid dynamics: a practical approach*. Elsevier.

[54] Kassem, H.I., Saqr, K.M., Aly, H.S., Sies, M.M., & Wahid, M.A. (2011). Implementation of the eddy dissipation model of turbulent non-premixed combustion in OpenFOAM. *International Communications in Heat and Mass Transfer*, 38(3), 363–367. doi: 10.1016/j.icheatmasstransfer.2010.12.012

[55] Kumaran K., & Babu, V. (2009). Investigation of the effect of chemistry models on the numerical predictions of the supersonic combustion of hydrogen. *Combustion and Flame*, 156(4), 826–841. doi: 10.1016/j.combustflame.2009.01.008

[56] Gerlinger, P., Stoll, P., Kindler, M., Schneider, F., & Aigner, M. (2008). Numerical investigation of mixing and combustion enhancement in supersonic combustors by strut induced streamwise vorticity. *Aerospace Science and Technology*, 12(2), 159–168. doi: 10.1016/j.ast.2007.04.003